

the magnetic field is aligned along the outflow direction. [Yen et al. \(2021\)](#) studied 62 low-mass Class 0 and I protostars in nearby (<450 pc) star-forming regions with the orientations of the magnetic fields on 0.05–0.5 pc scales. They suggest that the outflows are likely to be misaligned with B-fields by 50 degrees in 3D space. While [Hull & Zhang \(2019\)](#) used Atacama Large Millimeter/submillimeter Array (ALMA) observations with spatial resolutions of up to ~ 100 au, and conclude that magnetic fields and outflows are randomly aligned in low-mass protostellar cores. The discrepancy between simulations and observations can be due to the limitations of the simulation setup. As an example, [Lee et al. \(2017\)](#) applied an ideal magnetohydrodynamic (MHD) simulation when in reality non-ideal MHD effect might be important ([Wurster 2021](#)).

[Redaelli et al. \(2019a\)](#) used polarimetric observations of the dust thermal emission at 1.4THz obtained with the Stratospheric Observatory for Infrared Astronomy (SOFIA) telescope to investigate the magnetic field properties at the core scales toward IRAS15398. The authors found a uniform magnetic field consistent with the large-scale field derived from optical observations ([Franco & Alves 2015](#)). They suggested the core experienced a magnetically driven collapse and the core inherited the B-field morphology from the parental cloud during its evolution. The field lines pinch inward toward the central object, leading to the characteristic hourglass shape that is predicted by models of magnetically driven collapse. They showed that the mean direction of the magnetic field is aligned with the large-scale B-field and with the direction of outflow. Their prediction for a magnetic field strength of $B = 78 \mu\text{G}$ is expected to be accurate within a factor of two. They calculated the mass-to-flux ratio, $\lambda = 0.95$, which means that the core is in a state of transition between supercritical and subcritical states.

In this paper we present new observational data that allow us to study the gas kinematics, which we compare to the magnetic field direction. The aim is to assess the importance of magnetic fields in the dynamical evolution of low-mass star-forming regions. The outline of the paper is as follows. The observations and results are described in detail in Sects. 2 and 3. In Sect. 4 we analyze the observed line profiles of C^{18}O (2-1) and DCO^+ (3-2) emission lines. The results are summarized in Sect. 5.

2. Observations

2.1. APEX

IRAS15398 was observed using the Atacama Pathfinder EXperiment (APEX) single-dish antenna located at Llano de Chajnantor in the Atacama desert of Chile on 2019 September 14, 16, 17, 21, and 23. We used the PI230 receiver coupled with the FTS4G backend in the on-the-fly mode. We used the highest spectral resolution that the FTS4G could provide, 62.5 kHz ($\approx 0.08 \text{ km s}^{-1}$ at the frequency of the DCO^+ (3-2) line). The data were reduced to a pixel size of 9 arcsec. The broad bandwidth of the PI230 receiver can be set up to observe simultaneously C^{18}O (2-1) and the DCO^+ (3-2) transitions at 219.560 GHz and 216.113 GHz, respectively, the target lines of this research. The angular resolution at these frequencies is ~ 28 arcsec, corresponding to 0.02 pc at the source distance 156 pc ([Dzib et al. 2018](#)). The data reduction was performed based on the standard procedure of the CLASS software, GILDAS.¹ The antenna temperature, T_A , was converted to main-beam brightness tempera-

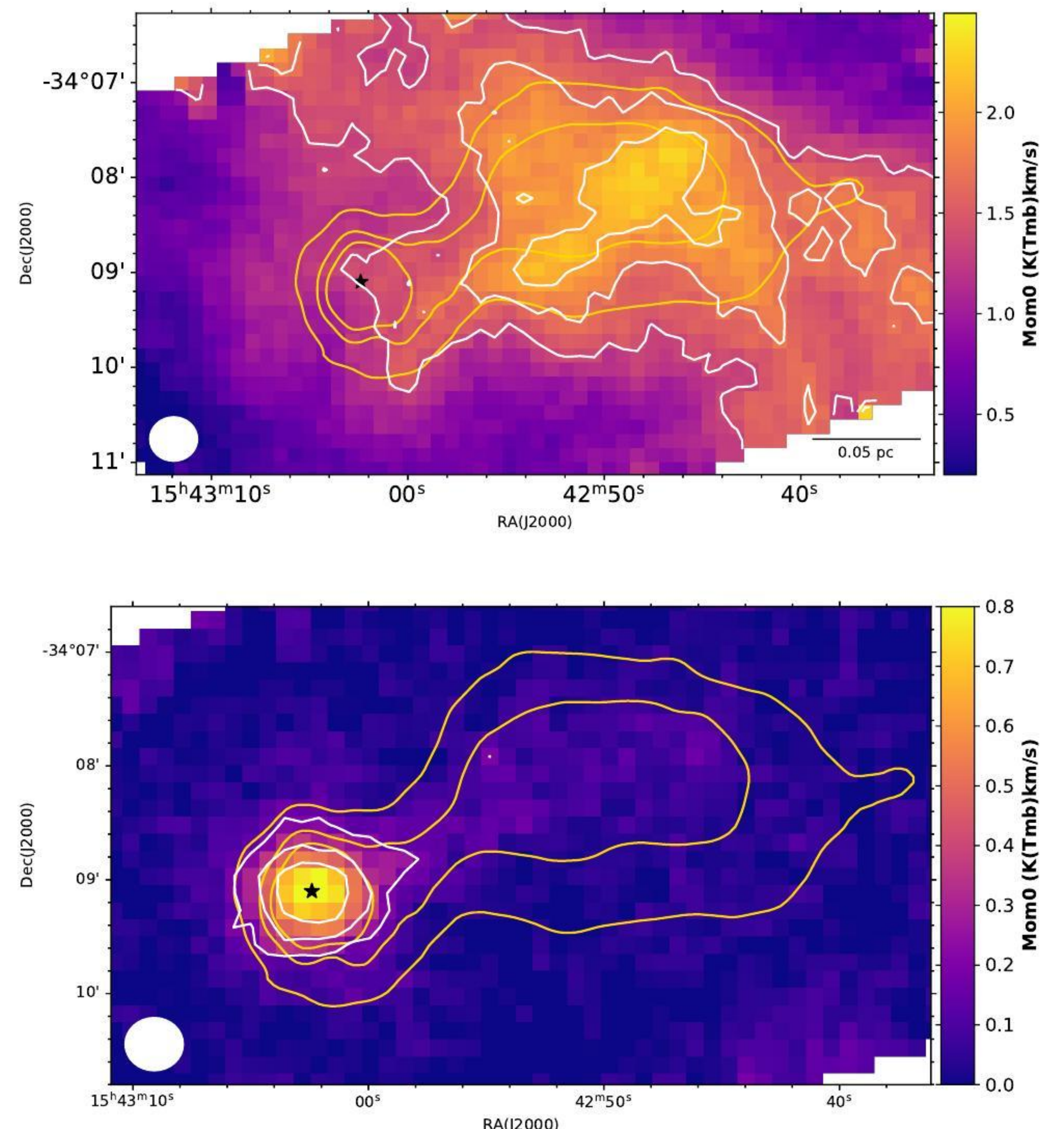


Fig. 1: Integrated intensity of C^{18}O (1-2) (top) and DCO^+ (3-2) (bottom) toward IRAS15398. The white contour levels are 10, 20, and 30 times of mean rms value for the DCO^+ line and 40, 50, and 60 times of mean rms value for the C^{18}O (2-1) line. The beam size is shown in the bottom left corner. The yellow contours in both images show H_2 column density (levels: [1.0, 1.5, 2.0] 10^{22} cm^{-2}). The black star gives the position of the protostar.

ture using the forward efficiency (η_{fw}) and main beam efficiency, $T_{\text{mb}} = T_A \frac{\eta_{\text{fw}}}{\eta_{\text{mb}}}$, given a main beam efficiency $\eta_{\text{mb}} = 0.8$.²

2.2. Herschel

We used archival data from the Gold Belt Survey, obtained with the *Herschel* space telescope to obtain the gas column density and the dust temperature ([Bontemps et al. 2010](#), [Rygl et al. 2013](#), [Benedettini et al. 2018](#)). The $\text{N}(\text{H}_2)$ column density map has a resolution of ~ 38 arcsec.

3. Result

Figure 1 presents the moment 0 (integrated intensity) maps of C^{18}O (2-1) and DCO^+ (3-2) overlaid with the contours of H_2 column density. The mean rms in T_{mb} scale is 0.1 K and 0.08 K for C^{18}O (2-1) and DCO^+ (3-2), respectively. On the basis of emission-free channels only, we derived the mean rms per channel for each transition. This rms is used to associate uncertainties at each pixel to the integrated intensity, the mean value for C^{18}O (2-1) and DCO^+ (3-2) being 0.03 K km s^{-1} and 0.02 K km s^{-1} , respectively. These lines are optically thin and do not present crowded hyperfine structures. In order to confirm this hypothesis, we evaluate the opacity as

$$\tau = -\ln \left[1 - \frac{T_{\text{MB}}}{J_{\nu}(T_{\text{ex}}) - J_{\nu}(T_{\text{bg}})} \right], \quad (1)$$

¹ <https://www.iram.fr/IRAMFR/GILDAS/>

² www.apex-telescope.org/telescope/efficiency/